Results in Engineering 24 (2024) 102981

Contents lists available at ScienceDirect

Results in Engineering

journal homepage: www.sciencedirect.com/journal/results-in-engineering

Development and wear resistivity performance of SiC and TiB_2 particles reinforced novel aluminium matrix composites

Abhijit Bhowmik [a,b], Binayak Sen [c,d], N. Beemkumar [e], Jasgurpreet Singh Chohan [f,g], Pardeep Singh Bains [h], Gurpartap Singh [i], Ambati Vijay Kumar [j], Johnson Santhosh A [k,*]

[a] Department of Mechanical Engineering, Dream Institute of Technology, Kolkata, 700104, India
[b] Centre of Research Impact and Outreach, Chitkara University, Rajpura, 140417, Punjab, India
[c] Centre for Computational Modeling, Chennai Institute of Technology, Chennai, Tamil Nadu, 600069, India
[d] Department of Mechanical Engineering, Chennai Institute of Technology, Chennai, Tamil Nadu, 600069, India
[e] Department of Mechanical Engineering, School of Engineering and Technology, JAIN (Deemed to Be University), Bangalore, Karnataka, India
[f] School of Mechanical Engineering, Rayat Bahra University, Kharar, Punjab, 140103, India
[g] Faculty of Engineering, Sohar University, PO Box 44, Sohar, PCI 311, Oman
[h] Department of Mechanical Engineering, Vivekananda Global University, Jaipur, Rajasthan, 303012, India
[i] Department of Mechanical Engineering, Chandigarh Engineering College, Chandigarh Group of Colleges, Jhanjeri, Mohali, Punjab, 140307, India
[j] Department of Mechanical Engineering, Raghu Engineering College, Dakamarri, 531162, Andhra Pradesh, India
[k] Faculty of Mechanical Engineering, Jimma Institute of Technology, Jimma University, Jimma, Ethiopia

A R T I C L E I N F O

Keywords:
Stir casting
Aluminium matrix composite
SiC reinforcement
TiB_2 reinforcement
Tribological assessment

A B S T R A C T

The aerospace and automotive industries, in particular, rely heavily on aluminium matrix composites because of their exceptional strength-to-mass ratio and resistance to high temperatures. This study investigates the development and wear resistivity performance of Aluminium Matrix Composites (AMCs) reinforced with SiC and TiB_2 particles. The experimental work involved fabricating AMCs using Aluminium Alloy 7075 as the matrix material with varying weight percentages of SiC and TiB_2 reinforcements. Tribological tests were conducted under different conditions of applied load, sliding speed, and sliding distance to analyze the wear behavior of the composites. Results revealed that higher weight percentages of reinforcement led to lower wear rates, particularly at elevated sliding speeds. X-ray diffraction analysis confirmed the presence of SiC and TiB_2 particles in the composites. It is observed that greater applied loads caused greater wear rates, bigger grooves, and substantial frictional heat production, demonstrating a direct relationship between load weight and wear performance. The study indicated that sticky wear management lowered wear rates at longer sliding distances not abrasive wear at shorter distances. The significance of this study lies in its contribution to optimizing the composition of multiphase reinforced AMCs for enhanced wear resistance in various industrial applications.

1. Introduction

Composite materials epitomize a noteworthy leap forward in engineering, proffering augmented strength relative to conventional alloys, thus broadening their application spectrum across diverse sectors encompassing aircraft, automotive, infrastructure, medicine, and defense [1–3]. Nevertheless, the incorporation of ceramic particle agents attenuates the ductility of metal matrix composites. Notwithstanding, the diffusion of reinforcement particles fortifies composite materials, amplifying attributes such as fatigue strength and creep resistance [4–6]. The tribological and mechanical performance of aluminum metal matrix composites fortified with a plethora of reinforcements outstrip those of orthodox materials, conferring benefits such as reduced weight, improved strength, stiffness, and lower wear rates. The preparation of metal matrix composites (MMCs) involves various techniques such as stir casting, spray deposition, and squeeze casting, depending on factors like dispersing agents, grain size, and morphology [7–10]. Different types of reinforcement agents, including TiC, Al_2O_3, SiC, fly ash, B_4C,

* Corresponding author.
E-mail addresses: abhijitbhowmik90@gmail.com (A. Bhowmik), binayaksen@citchennai.net (B. Sen), n.beemkumar@jainuniversity.ac.in (N. Beemkumar), jaskhera@gmail.com (J. Singh Chohan), singhbainspardeep@gmail.com (P.S. Bains), gurpartap@cgc.ac.in (G. Singh), vijay.mech@raghuenggcollege.in (A.V. Kumar), johnson.antony@ju.edu.et (J.S. A).

https://doi.org/10.1016/j.rineng.2024.102981
Received 24 July 2024; Received in revised form 20 September 2024; Accepted 20 September 2024
Available online 23 September 2024

and TiB_2, are utilized based on prior research for specific applications in respective fields [11,12]. In various industries, including aerospace and energy, mechanical components often function under harsh conditions, such as elevated temperatures and heavy loads, which contribute to significant wear [13,14]. Gupta et al. [15] investigates and compares the high-temperature tribological properties of ilmenite-reinforced and boron carbide-reinforced LM13 aluminum alloy-based matrix composites. Using stir casting, the composites were reinforced with 5–15 wt% of either natural or covalently bonded particles. Results showed that both reinforcements improved hardness, wear resistance, and thermal stability, with boron carbide exhibiting slightly superior performance. Gupta et al. [16] investigates the wear behavior of aluminum matrix hybrid composites reinforced with ilmenite ($FeTiO_3$) and boron carbide (B_4C) particles. Babu et al. [17] explores the development of hybrid composites based on AA 2014 alloy reinforced with Zirconium Diboride (ZrB_2) and Boron Carbide (B_4C), achieving improved hardness, tensile strength, and wear resistance through liquid metallurgy stir casting and varying reinforcement weight percentages. Pradeep et al. [18] investigates the fabrication of basalt fiber-reinforced composites with silicon dioxide (SiO_2) nanofillers, enhancing mechanical properties, hardness, and wear resistance. He et al. [19] synthesized using in-situ autogenous methods to improve the high-temperature friction and wear properties of aluminum alloys. Characterization and testing revealed significant wear resistance, especially at 100 °C, due to hard particles, oxide film, and self-lubricating effects. The nanofillers improved flexural strength, tensile strength, and wear resistance, with detailed analysis of fracture mechanisms using FESEM. By varying reinforcement loading and particle ratios, the study aims to assess the impact on wear resistance, friction, and microstructural changes under varying operating conditions using ASTM G99 standar Research conducted by Poria et al. [20] delved into the wear dynamics of TiB_2 particle-reinforced LM4 aluminum matrix composites, elucidating a decline in wear rate concomitant with escalated reinforcement content, juxtaposed against an increment with augmented load and sliding velocity. Sahin [21] undertook a comprehensive characterization of SiC powder-reinforced aluminum matrix composites, unveiling a uniform dispersion pattern and augmented hardness concomitant with SiC integration. Yadav and Dixit [22] conducted a detailed examination of the wear behavior of AA356 aluminum matrix composites reinforced with SiC and TiB_2, finding that composites enhanced with TiB_2 exhibited a significantly lower rate of mass depletion. Similarly, Bhowmik et al. [23] explored the mechanical properties and fracture resilience of Al7075 aluminum matrix composites reinforced with SiC/TiB_2 ceramic particulates, revealing that formulations fortified with TiB_2 demonstrated superior strength metrics compared to their SiC counterparts. Furthermore, Dey et al. [24] provided insights into the mechanical characteristics and wear behavior of Al2024 aluminum matrix composites dispersed with SiC/TiB_2, reporting increased tensile strength, higher hardness indices, and a reduced wear rate for the reinforced composites, as opposed to their unfortified equivalents.

In a series of studies, researchers have explored the impact of various reinforcement materials on the properties of aluminum matrix composites. Rao and Das [25] found that increasing the SiC content led to a decrease in wear rate and an increase in the coefficient of friction. Pazhouhanfar and Eghbali [26] studied Al6061 aluminum matrix composites reinforced with TiB_2 particles, noting improvements in tensile strength, flexural strength, and microhardness with higher TiB_2 content. Akbari et al. [27] focused on A356 aluminum matrix composites reinforced with TiB_2 particulates, observing enhanced tensile strength, toughness, and ductility with increased TiB_2 content. Wang et al. [28] meticulously scrutinized the microstructural intricacies of in-situ TiB_2 dispersed aluminum matrix composites, highlighting the nuanced uniformity in the distribution of TiB_2 particles and elucidating the pivotal role played by Al_3Ti intermetallic compounds in augmenting the efficacy of TiB_2 reinforcement mechanisms. Prasad et al. [29] embarked on a comprehensive inquiry into the wear and mechanical characteristics of aluminium composites featuring SiC/TiB_2 particulate reinforcements, discerning that the incorporation of TiB_2 engendered heightened levels of hardness and wear resilience vis-à-vis SiC counterparts. Meanwhile, Chen et al. [30] delved deep into the microstructural nuances and mechanical dynamics of TiB_2 particle-reinforced aluminum matrix composites, noting substantial enhancements in both tensile strength and hardness attributes. Lakshmikanthan et al. [31] expounded upon the microstructural intricacies, tribological behavior, and mechanical attributes of silicon carbide-reinforced metal matrix composites, accentuating the pervasive uniformity in SiC dispersion within the matrix, and consequently heralding improvements in hardness, and tensile strength. Ma et al. [32], in their investigation, meticulously analyzed the mechanical robustness, and microstructural distribution of TiB_2-reinforced aluminium matrix composites, delineating a predominantly uniform dispersion pattern albeit with localized agglomeration phenomena, alongside a noteworthy 7.75 % amplification in ultimate tensile strength (UTS) relative to their unreinforced alloy counterparts. Lastly, Ye et al. [33] delved into the ramifications of SiC reinforcement on the mechanical integrity of aluminum matrix composites, elucidating a discernible surge in yield strength concomitant with the incorporation of SiC particles, thus underscoring the consequential role played by reinforcement agents in augmenting material properties.

The extensive literature review on AMCs reinforced with SiC and TiB_2 particles reveals a significant focus on their mechanical properties, and microstructural characteristics. However, a noticeable gap emerges in the exploration of tribological characteristics of SiC and TiB_2 reinforced aluminium matrix composites. While individual studies have delved into the enhancements brought by each type of reinforcement separately, a comprehensive investigation of the effects of SiC and TiB_2 particles remains scarce. This study aims to bridge this gap by systematically analyzing the performance of AMCs with SiC and TiB_2 reinforcements, thereby providing valuable insights into the potential applications of these composites. The impact of this inquiry lies in its potential to offer a complete understanding of how the presence of SiC and TiB_2 can influence the tribological characteristics of AMCs. Such knowledge is essential for guiding the tailored design and development of advanced composite materials for various industrial sectors, including aerospace, automotive, and infrastructure, where lightweight, high strength and durability are paramount requirements. By elucidating the effects of the reinforced particles, this study aims to contribute to the optimization and innovation of AMC formulations for specific engineering applications, thus advancing the frontier of composite materials technology.

2. Materials and methods

2.1. Material selection

In the pursuit of crafting high-quality aluminium matrix composites, the alloy of choice for this investigation was Aluminium Alloy 7075 (Al7075), esteemed for its profound mechanical attributes, inherent ductility, and robust strength-to-toughness ratio, rendering it

Table 1
Chemical composition of Al7075.

Elements	Amount (Wt. %)
Cr	0.21
Fe	0.22
Si	0.04
Mg	2.58
Mn	0.03
Cu	1.65
Zn	5.75
Ti	0.03
Al	Balance

indispensable across structural and aerospace domains. The elemental composition of the Al7075 alloy is meticulously delineated in Table 1. In the quest for optimal reinforcement, equitably distributed weight percentages (3, 5, 7, and 9 wt%) of SiC and TiB2 were judiciously selected as reinforcement particulates. These reinforcement materials, as depicted in Table 2, possess commendable physical properties. SiC arises from the carbon-silicon amalgamation, forged through the crucible of extreme temperature electro-chemical reactions involving carbon and sand. Meanwhile, TiB_2 stands as a stalwart ceramic reinforcement agent renowned for its exceptional thermal conductivity, oxidative resilience, and formidable resistance to mechanical wear. SiC and TiB_2 particle-reinforced composites have found widespread utility across an array of applications, ranging from aircraft structures to mould tool manufacturing and structural deployments, courtesy of their enviable weight-to-strength ratios, diminished wear proclivities, and elevated resistance to creeping phenomena. The resultant composite formulations, tailored through the judicious manipulation of reinforcement type and weight percentage, are comprehensively detailed in Table 3, delineating the nuanced variations therein.

2.2. Fabrication method

The stir casting technique stands out as a premier method for fabricating metal matrix composites within the realm of metallurgical practices. As illustrated in Fig. 1, the experimental setup for the stir casting process provides a visual depiction of its operational intricacies. This method finds application in the melting of diverse metals such as aluminium, magnesium, and copper, offering notable advantages in terms of both cost-effectiveness and superior homogeneity of mixing compared to alternative fabrication methodologies. In the execution of this process, a crucible crafted from graphite cradles the Al7075 alloy block, subject to continuous heating via an induction furnace operating at a predetermined temperature. Prior to the introduction of reinforcements into the molten aluminium matrix, the reinforcements undergo preheating within a furnace (muffle) at a constant temperature to eliminate any oxides of surfaces. Subsequently, a permanent mould constructed from mild steel is employed to facilitate the pouring of the molten composite, with the mould preheated beforehand to mitigate issues of shrinkage and porosity. A comprehensive breakdown of the process parameters associated with the stir casting fabrication method is presented in Table 4, offering invaluable insights into its operational intricacies. To optimize wettability, an initial admixture of 2 wt% magnesium powder is introduced into the molten matrix material, thereby fostering robust bonding by reducing the surface energy (wetting angle) between the matrix alloy and the reinforcement particles. Moreover, the incorporation of pure magnesium serves to augment the fluidity of the molten metal, further enhancing the casting process. The resulting casted composites are visually showcased in Fig. 2, encapsulating the culmination of the stir casting process.

2.3. Tribological test

Dry sliding pin-on-disc tests were conducted using DUCOM's TR 20LE-M5 model, illustrated in Fig. 3. Specimens were meticulously machined to produce cylindrical pins measuring 6 mm in diameter and 40 mm in length. These pins were subsequently subjected to sliding contact against an EN31 steel disc with a hardness rating of 62 HRC. The

Table 2
Physical properties of reinforcement particles.

Reinforcement	SiC	TiB_2
Melting point	2730 °C	3230 °C
Purity	99.92 %	99 %
Density	3.21 gm/cc	4.52 gm/cc
Grain size	20 μm	13–14 μm

Table 3
List of casted composites.

Sl. No.	Matrix	Reinforcement	Wt.% of reinforcement	Composite Name (Given)
1	Al7075	None	0	A-0
2	Al7075	SiC	3	AS-3
3	Al7075	TiB_2	3	AT-3
4	Al7075	SiC	5	AS-5
5	Al7075	TiB_2	5	AT-5
6	Al7075	SiC	7	AS-7
7	Al7075	TiB_2	7	AT-7
8	Al7075	SiC	9	AS-9
9	Al7075	TiB_2	9	AT-9

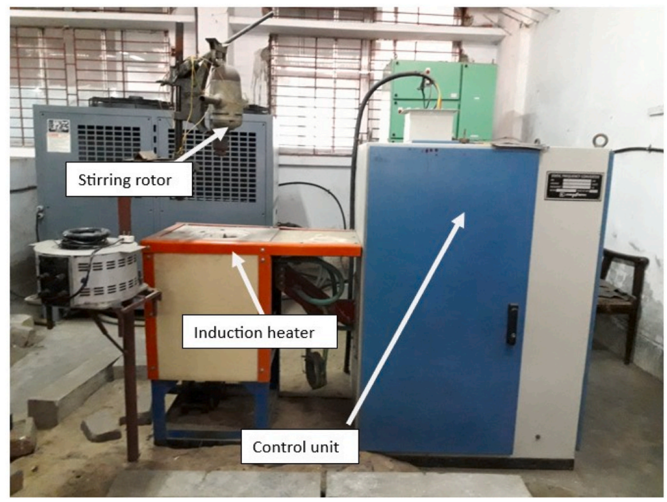

Fig. 1. The experimental configuration employed in the stir-casting.

tribological testing parameters, in accordance with ASTM G-99 standards, are comprehensively detailed in Table 5. The selection of reinforcement levels (3, 5, 7, and 9 wt%) was predicated on the presence of certain uncontrolled process parameters that have been observed to exacerbate issues such as porosity, clustering, slag incorporation, and crack formation within the casted composites. Moreover, exceeding the 9 wt% threshold for SiC and TiB_2 addition into the matrix has been found to compromise the strength of the resulting composite. Applied load levels (10, 20, 30, and 40 N) were chosen based on insights gleaned from prior research [34] endeavors, aimed at elucidating the influence of applied load on the wear rate of composite materials. Similarly, sliding velocity levels (0.5, 1, 1.5, and 2 m/s) were carefully determined to ensure the preservation of the contact surface, thereby mitigating the likelihood of surface damage. Notably, a sliding velocity of 3 m/s was deliberately omitted due to the potential formation of a thick oxide layer within the contact region, owing to the abbreviated contact period between the friction surfaces (pin and disc). Wear rate for specimen pin are calculated by using Eq. (1).

$$\text{Wear rate}\ (\text{mm}^3/\text{m}) = \frac{\text{Volumetric Loss}}{\text{Sliding Distance}} \tag{1}$$

3. Results and discussions

3.1. X-ray diffraction analysis

X-ray Diffraction (XRD) stands as the preeminent technique employed for the determination of elemental composition within composite specimens, discernible through the emergence of distinctive peaks. Employing a Cu-Kα radiation source, the XRD graph is meticulously crafted by a specialized X-ray Diffractometer, with a 2θ range

Table 4
Details concerning the process parameters utilized in the stir-casting technique.

Parameters	Stirring speed	Stirring time	Stirring temperature	Preheat temperature of the mould	Preheat temperature of reinforcement
Unit	rpm	minute	°C	°C	°C
Value	300	10	750	400	450

meticulously selected spanning from 10° to 70°. Illustrated in Fig. 4 is the XRD pattern delineating the composition of a composite matrix comprising particulates of SiC and TiB_2 reinforcing an aluminum substrate. Upon scrutiny of the XRD spectrum, it becomes apparent that the incorporation of SiC-reinforced aluminum matrix composites (denoted as AS-3, AS-5, AS-7, and AS-9) manifests in the emergence of six prominent peaks. Among these, three prominent peaks correspond to aluminum (Al), with 2θ values registering at 38.45°, 44.79°, and 66.24°, while two others signify the presence of SiC at 35.18° and 54.61°, with the final peak attributed to magnesium silicon (Mg_2Si) appearing at 40.22°. Similarly, the integration of TiB_2-reinforced aluminum matrix composites (termed AT-3, AT-5, AT-7, and AT-9) is characterized by six notable peaks. Mirroring the pattern observed in SiC-reinforced variants, three peaks are ascribed to aluminum (Al), aligning precisely with 2θ values of 38.45°, 44.79°, and 66.24°. Additionally, two peaks emerge indicative of the presence of TiB_2 at 30.57° and 62.52°, while the remaining peak signifies the presence of titanium aluminide (Al_3Ti) at 27.76°.

3.2. Wear analysis

3.2.1. Effect of applied load

Wear tests are conducted to assess the wear rate of materials, thereby aiding in the determination of their suitability for specific applications involving wear. Illustrated in Fig. 5 is the wear resistance behavior exhibited by aluminum matrix composites reinforced with SiC and TiB_2, under varying loads (10, 20, 30, and 40N), while maintaining a constant sliding speed of 1 m/s and a sliding distance of 1000 m. The wear rate escalates notably with increasing applied load during sliding, precipitating a discernible impact on the size distribution of wear debris and the topography of the worn surface of the specimen. Initially, the hard asperities of the counter plate trench the softer pin surface of the composite, displacing its micro-asperities, and subsequently, during sliding, embedding these displaced asperities into the counter plate, thereby progressively augmenting adhesion. Ensuing each experimental iteration, it becomes imperative to address the adherence of the softer pin surface to the counter plate. Notably, the wear rate of the unreinforced aluminum matrix 7075 is significantly elevated compared to its reinforced counterparts. This phenomenon can be attributed to two primary factors: the introduction of SiC and TiB_2 reinforcement particulates, bolstering the mechanical properties of the composite, and the concurrent formation of oxides coupled with strain hardening [35–37]. The applied load exerts a pivotal influence on the stress experienced within the interaction zone between the pin and disc, exacerbating the generation of frictional heat. This additional heat elevates the temperature of the exposed surface, facilitating oxide formation, which, in turn, fortifies surface hardness. The presence of metallic oxides serves as a salient mechanism for mitigating wear rates. Elevated loads distort pin asperities, fostering the formation of a contiguous surface layer, thereby escalating pin surface temperatures. This rise in temperature precipitates wear loss and initiates the development of a tribo-layer, pivotal for diminishing wear rates over prolonged sliding cycles. Abrasive wear is exacerbated under heavy loads, resulting in the generation of wear debris interspersed between the sliding surfaces. Conversely, at lower loads, abrasive wear diminishes, culminating in shallower grooves owing to the inherent hardness conferred by SiC and TiB_2 particulates distributed throughout the matrix. Notably, the Al7075/9 wt%TiB_2 (AT-9) aluminum matrix composite exhibits minimal wear compared to its counterparts, attributed to its heightened hardness. Fig. 6 illustrates the variation of the coefficient of friction (COF) across the range of applied loads. Notably, the COF tends to decrease with increasing load, attributable to the developmental dynamics between pin and disc surfaces, characterized by a cyclic progression of development, distortion, destruction, and reformation, compounded by the proliferation of contact asperities [38]. Temperature augmentation with increasing load fosters the development of a smoother molten surface at contact asperities, consequently reducing shear stress and, in turn, the coefficient of friction [39]. Elevated temperatures also facilitate the construction of a thick oxide layer, further ameliorating adhesion and decreasing the coefficient of friction [40].

Dry sliding worn surface micrographs of composite pins rotating against the counter plate under varying loads (10, 20, 30, and 40N), with a consistent sliding speed of 1 m/s and sliding distance of 1000 m, are depicted for AS-9 and AT-9 alloy composites in Fig. 7(a–h). These composites boast the highest content (9 wt%) of SiC and TiB_2 particles. The transition of harder asperities into abrasive particles initiates a three-body abrasive wear mechanism, characterized by plowing and micro-cutting actions, as evident from the worn surface micrographs. Accumulated wear debris exacerbates abrasive wear, contributing to material loss from the surface. The presence of porosity within the composite structure acts as a stress concentrators, precipitating localized strain concentrations within the pin surface. These regions of heightened strain serve as nucleation sites for crack initiation and propagation, resulting in extensive surface damage and wear loss, particularly observable in Fig. 7(a). Micrographs of the worn surface also reveal the presence of unstructured craters, indicative of delamination mechanisms occurring during abrasion. The pressure exerted between the pin and disc leads to the fracture of pin asperities, generating debris that manifests as small indentations or "ditches" on the worn surface, as illustrated in Fig. 7(b). Upon subsequent rubbing under a 20 N applied load, the same reinforced composite exhibits an elevated wear rate. Fig. 7(d) showcases the formation of larger grooves and the occurrence of frictional heating, leading to plastic deformation characteristic of adhesive wear [41,42]. Burned patches are also found at some higher amount of applied load (20N) depicted in Fig. 7(c and d). A secondary layer marked at a higher amount of applied load (30N) SiC reinforced composite is depicted in Fig. 7(e). The friction-layer surface development is minor as it retains on development-distortion-destruction-reformation mechanism due to the existence of harder asperities. At higher loads (40N), micro-cutting and cracks are also observed at the pin surface caused by dislocating of particles as shown in Fig. 7(g and h). As shown in Fig. 7(e, h) the primary surface is protected from sliding as there is visible to be minor secondary along with tribo-layers [41]. Harder asperities of counter disc surface are plowing the soft matrix and therefore reforms the plowing of the soft matrix generate cracks that extend axial and sideways, and deformation of the subsurface.

3.2.2. Effect of sliding speed

Fig. 8 illustrates the wear behavior of composites concerning the variation of sliding speed (0.5, 1, 1.5, and 2 m/s), while maintaining a constant applied load of 20N and a sliding distance of 1000m. A discernible trend emerges wherein the wear rate escalates proportionally with increasing sliding speed, attributable to the heightened coverage of distance over time. The sliding speed factor exerts a pronounced influence on the generation of frictional heat at the interface between the pin and disc. This thermal energy weakens the bond between the matrix and reinforcement components, precipitating shear

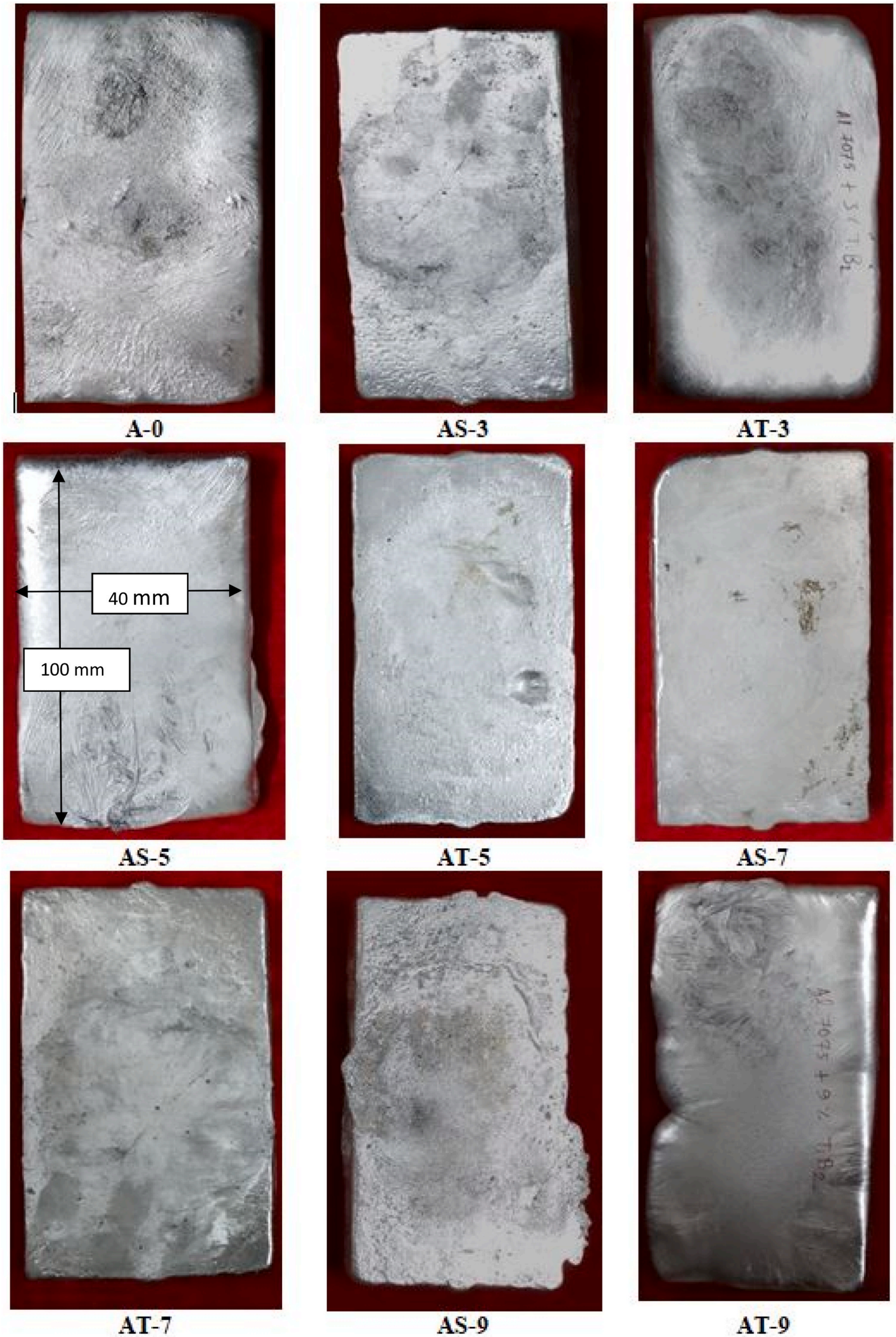

Fig. 2. Stir casted aluminium matrix composites.

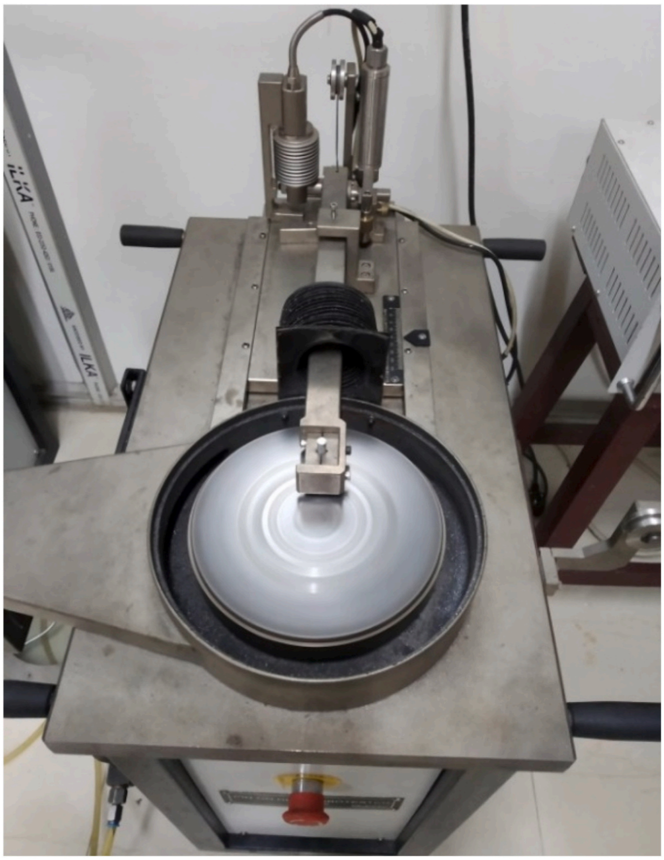

Fig. 3. The experimental setup for pin-on-disc wear testing.

Table 5
Specifications of the process parameters employed in the wear test.

Parameters	Load	Sliding speed	Pin diameter	Track diameter
Unit	N	m/s	mm	mm
Value	10, 20, 30 and 40	0.5, 1, 1.5 and 2	6	80

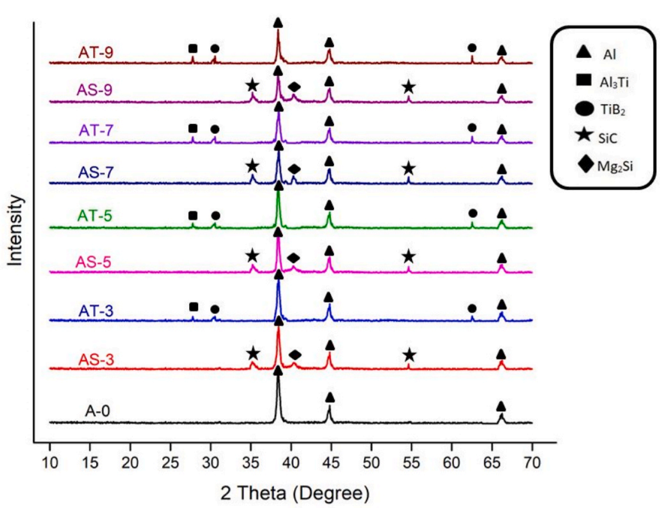

Fig. 4. XRD pattern of Al7075/SiC and Al7075/TiB_2 composite.

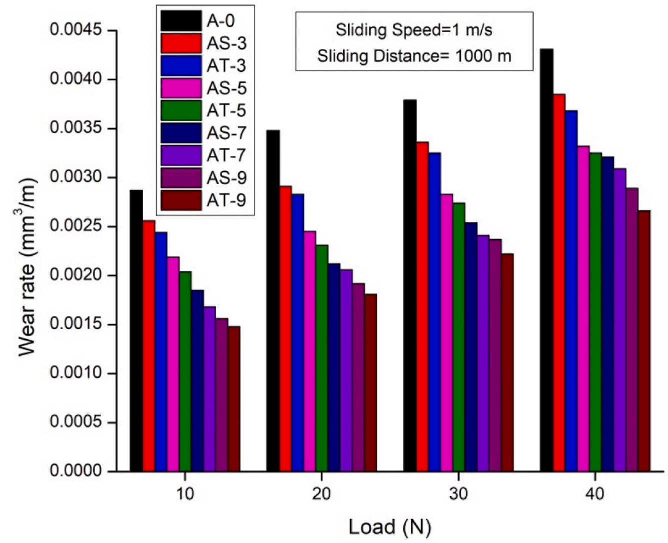

Fig. 5. A graphical depiction illustrating the variation in wear rate versus load, considering the reinforcements.

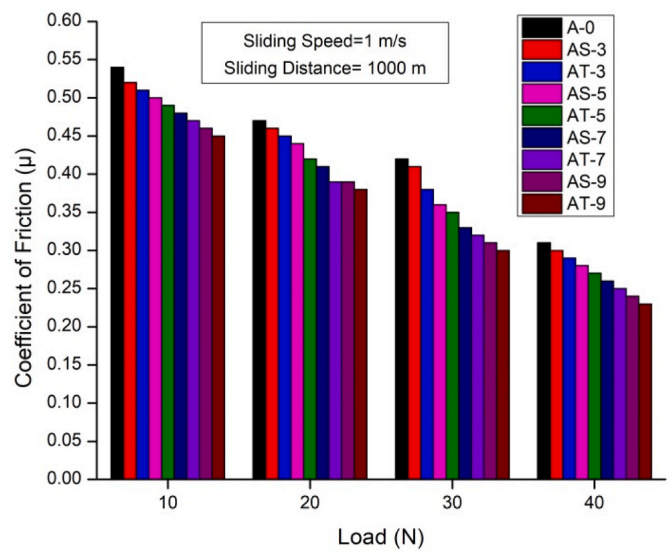

Fig. 6. A graphical representation depicting the variation of coefficient of friction versus load, considering the reinforcements.

forces that transform hard particles into wear debris, augmenting the contact surface among the pin as well as disc. Furthermore, it is observed that composites with higher weight percentages of reinforcement exhibit lower wear rates compared to their counterparts with lower weight percentages, particularly noticeable at elevated sliding speeds. At a fixed applied load, sliding speed emerges as the predominant factor influencing advanced shear forces. Delamination wear is primarily induced by maximum shear stress, leading to an escalation in wear loss at higher sliding speeds. Conversely, lower sliding speeds mitigate shear force generation, thereby reducing the removal of hard particles from the matrix and minimizing ploughing of the softer matrix material. Consequently, total wear loss is diminished at lower sliding speeds relative to higher speeds under a fixed load. Moreover, the escalation in sliding speed, while maintaining other parameters constant, engenders heightened heat generation at the contact point between the pin and disc, fostering the development of a mechanically mixed layer responsible for elevated wear rates. Fig. 9 delineates the behavior of the COF of composites in response to varying sliding speeds. The results

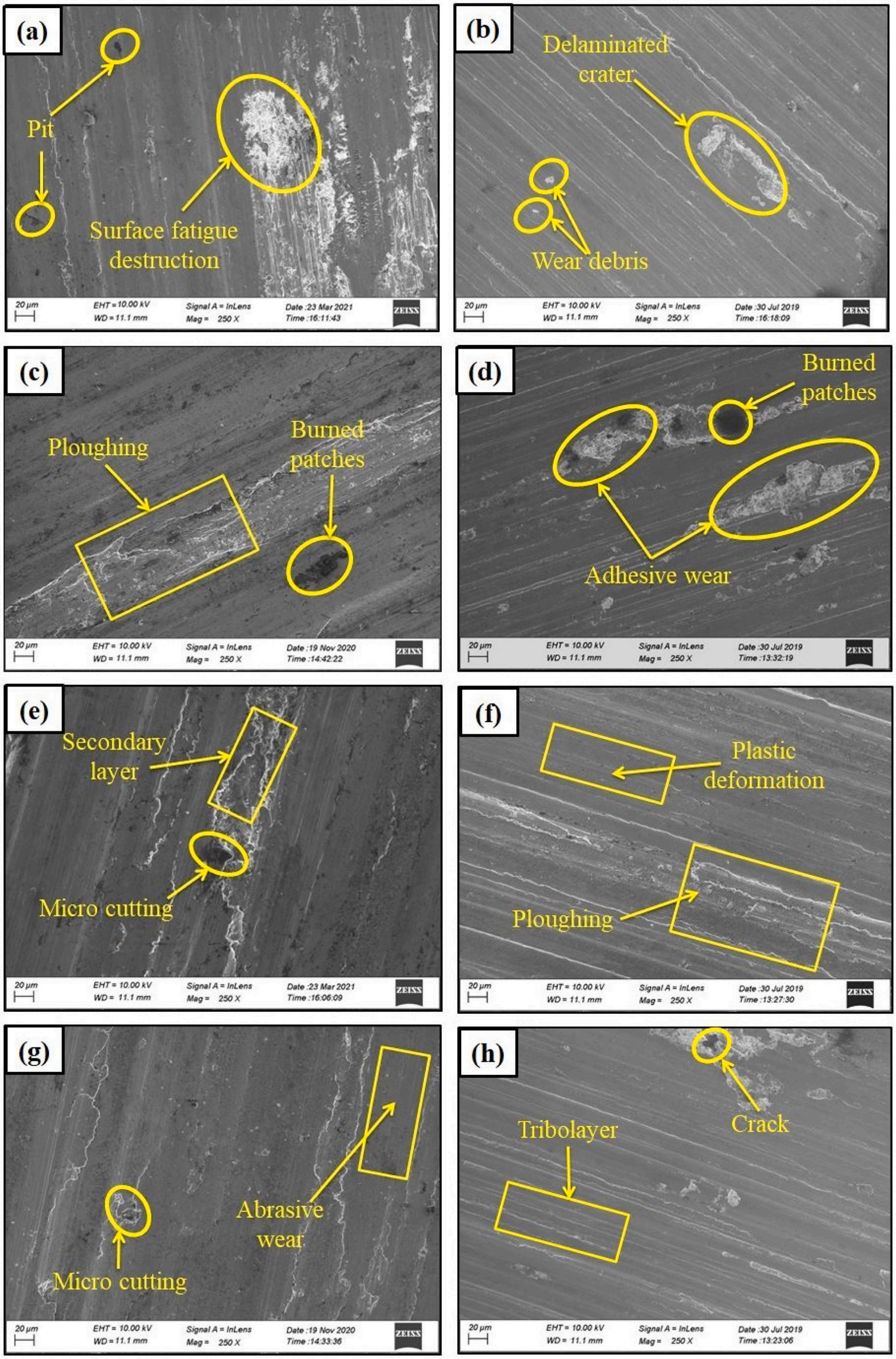

Fig. 7. Worn morphology: (a) AS-9 at 10N, (b) AT-9 at 10N, (c) AS-9 at 20N, (d) AT-9 at 20N, (e) AS-9 at 30N, (f) AT-9 at 30N, (g) AS-9 at 40N, (h) AT-9 at 40N.

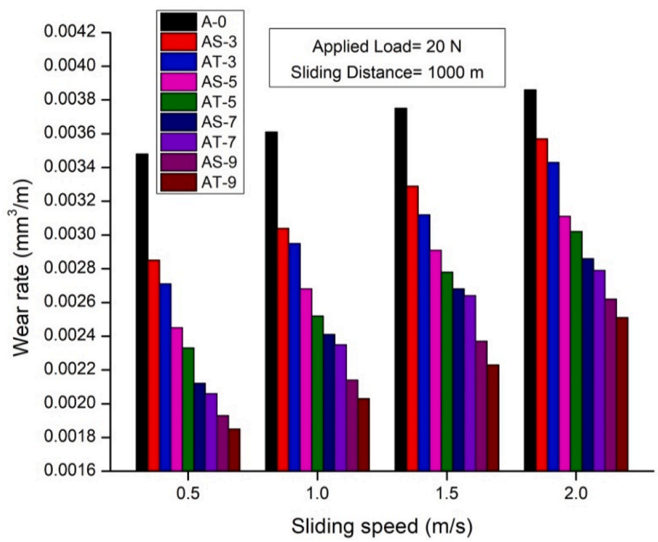

Fig. 8. A graphical representation illustrating the variation in wear rate versus sliding speed, considering the reinforcements.

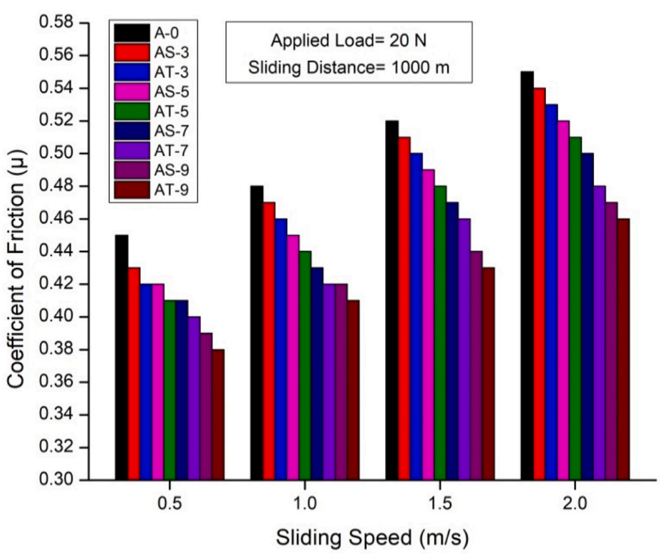

Fig. 9. A graphical representation depicting the variation of coefficient of friction versus sliding speed, considering the reinforcements.

demonstrate a progressive rise in the coefficient of friction (COF) as sliding speed increases. This phenomenon is attributed to the dynamic interplay of frictional layer formation, wear, and renewal at the contact interface between the pin and disc, a process accentuated with higher sliding speeds [43]. Additionally, the proliferation of interaction asperities at the contact point, coupled with the heightened presence of hard phases, amplifies frictional force, contributing to an expanded range of COF. Notably, the range of COF diminishes concurrently with the increasing weight percentage of hard reinforcements in the matrix for any specific speed factor. Experimentation discerns that unreinforced Al7075 alloy exhibits the maximum COF, recorded at 0.55 at 2 m/s sliding speed, while the Al7075/9%TiB_2 composite showcases the minimum COF, measured at 0.38 at 0.5 m/s sliding speed. The augmentation of friction between contact surfaces, attributed to the presence of hard phases, significantly augments frictional force.

The surface interactions between composite pins and the counter plate, subject to varying sliding speeds (0.5, 1, 1.5, and 2 m/s) under a constant load of 20N and sliding distance of 1000m, are visually captured in Fig. 10 for AS-9 and AT-9 alloy composites, boasting the highest content (9 wt%) of SiC and TiB_2 particles. The enhanced mechanical properties conferred by SiC and TiB_2 reinforcements bolster the endurance limit of material removal rates, as evidenced by the rubbing surfaces depicted in Fig. 10(f–h). Notably, with escalating sliding velocities while other parameters remain constant, a mechanically mixed layer (MML) manifests. This MML arises from the amalgamation of oxide surfaces immediately subsequent to critical plastic deformation of the rubbing surface at elevated temperatures, an outcome particularly pronounced at higher sliding velocities [44]. A conspicuous burnt spot discernible in Fig. 10(e, f) arises from the substantial flash temperatures generated at the contact surface during the traversal of extensive distances. Wear debris generated during sliding serves as abrasive particulates, intensifying abrasive wear and material removal from the surface, manifesting in the form of ploughing and pit development. Each worn micrograph reveals groove marks resultant from the rubbing of reinforcement particles in the sliding direction [45]. At higher sliding speeds, the worn morphology depicted in Fig. 10(g, h) showcases the presence of short pits, attributed to the impact of hard asperities from the counter plate or disc. The presence of voids acts as stress concentrators, culminating in significant strain accumulation and crack propagation across multiple void regions, thereby precipitating substantial surface damage and elevated wear rates. Delamination of the surface, pit formation, the presence of mechanically mixed layers, ploughing, abrasive wear, and crack formation in both axial and lateral directions are prominently observed, indicative of the generation of shear stress. Material loss is further exacerbated by the formation of wear debris resulting from crack propagation. Elevated frictional heat at higher sliding speeds leads to the softening of the pin surface, thereby reducing material strength. The presence of harder reinforcement particles within the matrix fails to fully mitigate material losses at higher sliding speeds, potentially due to the softening of the material, which compromises its ability to retain hard particulates. Consequently, even minor shear forces can dislodge hard particulates from the matrix, contributing to increased material loss.

4. Conclusions

The study conducted a tribological assessment of various weighted multi-phase reinforced aluminium matrix composites under different conditions of applied load, sliding speed, and sliding distance. The investigation aimed to understand the wear mechanisms and behaviours of these composites to provide insights for improving their tribological performance. So, the following conclusions can be drawn from the study.

(a) The presence of unstructured craters, delamination mechanisms, and adhesive wear were observed in SiC reinforced aluminium matrix composites under varying applied loads, indicating significant surface damage and wear loss.
(b) Higher applied loads led to increased wear rates, larger grooves, frictional heat generation, and plastic deformation, highlighting the importance of load weight in tribological performance.
(c) Abrasive wear followed by adhesive wear was predominant in AS-9 and AT-9 composites at smaller sliding distances, while control of adhesive wear reduced wear rates at longer sliding distances.
(d) The formation of a thin secondary layer and friction film contributed to reducing wear rates in composites covering larger sliding distances, demonstrating the influence of sliding distance on wear behaviour.
(e) Sliding speed significantly impacted wear rates by increasing frictional heat generation, weakening the bond between matrix and components, and enhancing contact surfaces between the pin and disc.

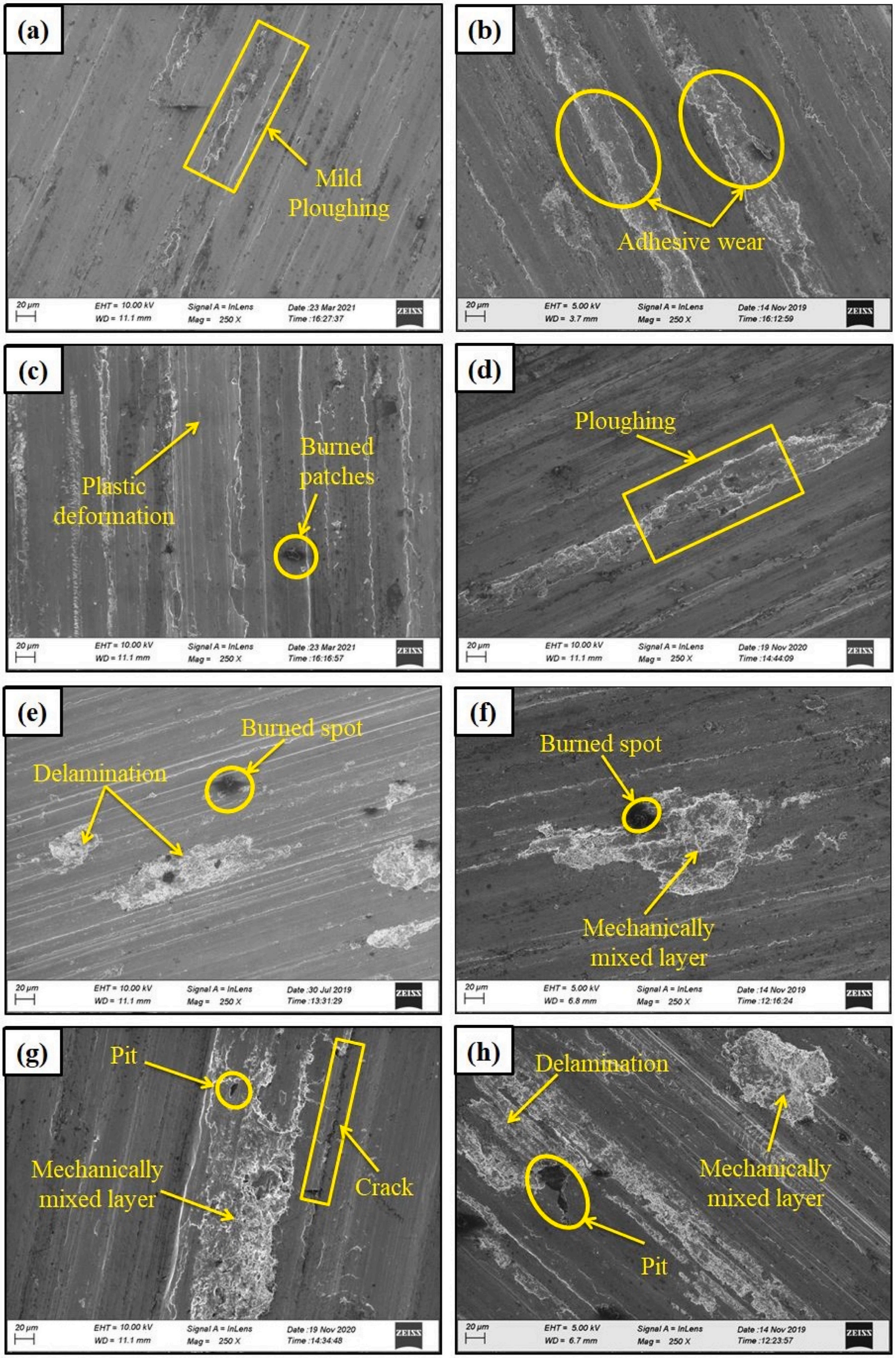

Fig. 10. Worn morphology: (a) AS-9 at 0.5 m/s, (b) AT-9 at 0.5 m/s, (c) AS-9 at 1 m/s, (d) AT-9 at 1 m/s, (e) AS-9 at 1.5 m/s, (f) AT-9 at 1.5 m/s, (g) AS-9 at 2 m/s, (h) AT-9 at 2 m/s.

The study opens avenues for further research in optimizing the composition of multi-phase reinforced aluminium matrix composites to enhance their wear resistance under varying tribological conditions. Future investigations could focus on exploring novel reinforcement materials, surface treatments, and lubrication techniques to mitigate wear mechanisms and improve the overall tribological performance of these composites. Additionally, studying the long-term durability and performance of these materials in real-world applications would provide valuable insights for industrial implementation.

Funding

Not applicable.

CRediT authorship contribution statement

Abhijit Bhowmik: Writing – original draft, Validation, Software, Methodology, Investigation, Formal analysis, Data curation, Conceptualization. **Binayak Sen:** Writing – review & editing, Writing – original draft, Validation, Software, Methodology, Formal analysis, Conceptualization. **N. Beemkumar:** Writing – review & editing, Software, Resources, Formal analysis. **Jasgurpreet Singh Chohan:** Writing – review & editing, Visualization, Supervision, Project administration, Conceptualization. **Pardeep Singh Bains:** Writing – review & editing, Visualization, Supervision, Project administration, Formal analysis, Data curation. **Gurpartap Singh:** Writing – review & editing, Validation, Methodology, Formal analysis, Conceptualization. **Ambati Vijay Kumar:** Writing – review & editing, Validation, Resources, Data curation, Conceptualization. **Johnson Santhosh A:** Writing – review & editing, Supervision, Project administration, Data curation, Conceptualization.

Declaration of competing interest

The authors declare that they have no known competing financial interests or personal relationships that could have appeared to influence the work reported in this paper.

Data availability

Data will be made available on request.

References

[1] P.S. Bains, S.S. Sidhu, H.S. Payal, Fabrication and machining of metal matrix composites: a review, Mater Manuf Processes 31 (5) (2016) 553–573.
[2] J. Jiang, Y. Wang, Microstructure and mechanical properties of the semisolid slurries and rheoformed component of nano-sized SiC/7075 aluminum matrix composite prepared by ultrasonicassisted semisolid stirring, Mater Sci Eng: A 639 (2015) 350–358.
[3] G. Moona, R.S. Walia, V. Rastogi, R. Sharma, Aluminium metal matrix composites: a retrospective investigation, Indian J. Pure Appl. Phys. 56 (2) (2018) 164–175.
[4] B. Kumar, J.V. Menghani, Aluminium-based metal matrix composites by stir casting: a literature review, Int J Mater Eng Innovation 7 (1) (2016) 1–14.
[5] H.R. Ezatpour, S.A. Sajjadi, M.H. Sabzevar, Y. Huang, Investigation of microstructure and mechanical properties of Al6061-nanocomposite fabricated by stir casting, Mater Design 55 (2014) 921–928.
[6] V.C. Uvaraja, N. Natarajan, K. Sivakumar, S. Jegadheeshwaran, S. Sudhakar, Tribological behavior of heat treated Al 7075 aluminium metal matrix composites, Indian J. Eng. Mater. Sci. 22 (1) (2015) 51–61.
[7] P.S. Reddy, R. Kesavan, B.V. Ramnath, Investigation of mechanical properties of aluminium 6061-silicon carbide, boron carbide metal matrix composite, Silicon 10 (2) (2018) 495–502.
[8] E. Jayakumar, A.P. Praveen, T.P.D. Rajan, B.C. Pai, Studies on tribological characteristics of centrifugally cast SiCp-reinforced functionally graded A319 aluminium matrix composites, Trans Indian Institute Metals 71 (11) (2018) 2741–2748.
[9] X. Liu, Y. Liu, D. Huang, Q. Han, X. Wang, Tailoring in-situ TiB2 particulates in aluminum matrix composites, Mater Sci Eng: A 705 (2017) 55–61.
[10] D. Bandhu, A. Thakur, R. Purohit, R.K. Verma, K. Abhishek, Characterization & evaluation of Al7075 MMCs reinforced with ceramic particulates and influence of age hardening on their tensile behavior, J. Mech. Sci. Technol. 32 (7) (2018) 3123–3128.
[11] S. Baskaran, V. Anandakrishnan, M. Duraiselvam, Investigations on dry sliding wear behavior of in situ casted AA7075–TiC metal matrix composites by using Taguchi technique, Mater Design 60 (2014) 184–192.
[12] R. Kumar, S. Dhiman, A study of sliding wear behaviors of Al-7075 alloy and Al-7075 hybrid composite by response surface methodology analysis, Mater Design 50 (2013) 351–359.
[13] R. Gupta, T. Nanda, O.P. Pandey, Tribological properties of hybrid aluminium matrix composites reinforced with boron carbide and ilmenite particles for brake rotor applications, Arch. Civ. Mech. Eng. 23 (1) (2022) 47.
[14] R. Gupta, S. Sharma, T. Nanda, O.P. Pandey, A comparative study of dry sliding wear behaviour of sillimanite and rutile reinforced LM27 aluminium alloy composites, Mater. Res. Express 7 (1) (2020) 016540.
[15] R. Gupta, T. Nanda, O.P. Pandey, V. Singhal, S. Bansal, R.S. Raman, Comparison of tribological characteristics of LM13/B4C and LM13/ilmenite composites at high-temperature conditions, J. Tribol. 146 (5) (2024).
[16] R. Gupta, T. Nanda, O.P. Pandey, Tribological characteristics of LM13 alloy based ilmenite-boron carbide reinforced hybrid composites for brake drum applications, Wear 522 (2023) 204851.
[17] C. Rajendran, A. Saiyathibrahim, R. Velu, Influence of B4C and ZrB2 reinforcements on microstructural, mechanical and wear behaviour of AA 2014 aluminium matrix hybrid composites, Defence Technology (2024).
[18] V. Pradeep, P. Kumar, I.R. Reddy, Investigation on mechanical properties and wear behavior of basalt fiber and SiO2 nanofillers reinforced composites, Results in Engineering 23 (2024) 102722.
[19] W. He, H. Li, X. Han, X. Wang, G. Wang, X. Zhang, O. Shcheretskyi, High-temperature dry sliding friction and wear behavior of in-situ (Al3Zr+ ZrB2)/AA6016 aluminum matrix composites, Mater. Today Commun. 39 (2024) 108951.
[20] S. Poria, P. Sahoo, G. Sutradhar, Tribological characterization of stir-cast aluminium-TiB2 metal matrix composites, Silicon 8 (4) (2016) 591–599.
[21] Y. Sahin, Preparation and some properties of SiC particle reinforced aluminium alloy composites, Mater Design 24 (8) (2003) 671–679.
[22] P.K. Yadav, G. Dixit, Erosive-corrosive wear of aluminiumsilicon matrix (AA336) and SiCp/TiB2p ceramic composites, Silicon 11 (3) (2019) 1649–1660.
[23] A. Bhowmik, D. Dey, A. Biswas, Comparative study of microstructure, physical and mechanical characterization of SiC/TiB2 reinforced aluminium matrix composite, Silicon (2020) 1–8.
[24] D. Dey, A. Biswas, Comparative study of physical, mechanical and tribological properties of Al2024 alloy and SiC-TiB2 composites, Silicon (2020) 1–12.
[25] R.N. Rao, S. Das, Effect of SiC content and sliding speed on the wear behaviour of aluminium matrix composites, Mater Design 32 (2) (2011) 1066–1071.
[26] Y. Pazhouhanfar, B. Eghbali, Microstructural characterization and mechanical properties of TiB2 reinforced Al6061 matrix composites produced using stir casting process, Mater Sci Eng: A 710 (2018) 172–180.
[27] M.K. Akbari, H.R. Baharvandi, K. Shirvanimoghaddam, Tensile and fracture behavior of nano/micro TiB2 particle reinforced casting A356 aluminum alloy composites, Mater Design 66 (2015) 150–161, 1980–2015.
[28] X. Wang, R. Brydson, A. Jha, J. Ellis, Microstructural analysis of Al alloys dispersed with TiB2 particulate for MMC applications, J Microscopy 196 (Pt 2) (1999) 137–145.
[29] V.J. Prasad, K.N. Rao, N.K. Babu, Mechanical and tribological characterization of aluminum metal matrix composite reinforced with micro ceramic particles (TiB2/SiC), Mater Today: Proceed 23 (2020) 637–641.
[30] F. Chen, Z. Chen, F. Mao, T. Wang, Z. Cao, TiB2 reinforced aluminum based in situ composites fabricated by stir casting, Mater Sci Eng: A 625 (2015) 357–368.
[31] A. Lakshmikanthan, S. Bontha, M. Krishna, P.G. Koppad, T. Ramprabhu, Microstructure, mechanical and wear properties of the A357 composites reinforced with dual sized SiC particles, J Alloys Compounds 786 (2019) 570–580.
[32] S. Ma, Y. Wang, X. Wang, Microstructures and mechanical properties of an Al-Cu-Mg-Sc alloy reinforced with in-situ TiB2 particulates, Mater Sci Eng A (2020) 139603.
[33] T. Ye, Y. Xu, J. Ren, Effects of SiC particle size on mechanical properties of SiC particle reinforced aluminum metal matrix composite, Mater Sci Eng: A 753 (2019) 146–155.
[34] V. Kaushik, A. Aherwar, A. Sharma, S. Kumar, S. Aftab, R. Khargotra, T. Singh, Influence of cow dung ash and TiB2 on the physicomechanical and tribological performance of Al6061-based hybrid composites, Results in Engineering 19 (2023) 101311.
[35] L. Jiang, H. Yang, J.K. Yee, X. Mo, T. Topping, E.J. Lavernia, J.M. Schoenung, Toughening of aluminum matrix nanocomposites via spatial arrays of boron carbide spherical nanoparticles, Acta Mater. 103 (2016) 128–140.
[36] Ş. Karabulut, H. Karakoç, R. Çıtak, Influence of B4C particle reinforcement on mechanical and machining properties of Al6061/B4C composites, Compos. B Eng. 101 (2016) 87–98.
[37] T. Hariprasad, K. Varatharajan, S. Ravi, Wear characteristics of B4C and Al2O3 reinforced with Al 5083 metal matrix based hybrid composite, Procedia Eng. 97 (2014) 925–929.
[38] S. Zhiqiang, Z. Di, L. Guobin, Evaluation of dry sliding wear behavior of silicon particles reinforced aluminum matrix composites, Materials & design 26 (5) (2005) 454–458.
[39] B. Bhushan, Tribology and Mechanics of Magnetic Storage Devices, Springer Science & Business Media, 2012.
[40] S.A. Kori, T.M. Chandrashekharaiah, Studies on the dry sliding wear behaviour of hypoeutectic and eutectic Al–Si alloys, Wear 263 (1–6) (2007) 745–755.

[41] R.N. Rao, S. Das, D.P. Mondal, G. Dixit, Mechanism of material removal during tribological behaviour of aluminium matrix (Al–Zn–Mg–Cu) composites, Tribol. Int. 53 (2012) 179–184.
[42] A. Vencl, I. Bobic, S. Arostegui, B. Bobic, A. Marinković, M. Babić, Structural, mechanical and tribological properties of A356 aluminium alloy reinforced with Al2O3, SiC and SiC+ graphite particles, J. Alloys Compd. 506 (2) (2010) 631–639.
[43] P. Sharma, K. Paliwal, R.K. Garg, S. Sharma, D. Khanduja, A study on wear behaviour of Al/6101/graphite composites, Journal of Asian ceramic societies 5 (1) (2017) 42–48.
[44] S. Baskaran, V.A. Anandakrishnan, M. Duraiselvam, Investigations on dry sliding wear behavior of in situ casted AA7075–TiC metal matrix composites by using Taguchi technique, Mater. Des. 60 (2014) 184–192.
[45] S. Sardar, S.K. Pradhan, S.K. Karmakar, D. Das, Modeling of abraded surface roughness and wear resistance of aluminum matrix composites, J. Tribol. 141 (7) (2019).